

North American winter-spring storms: Modeling investigation on tropical Pacific sea surface temperature impacts

Soumik Basu,¹ Xiangdong Zhang,¹ Igor Polyakov,¹ and Uma S. Bhatt²

Received 8 August 2013; revised 18 September 2013; accepted 20 September 2013; published 3 October 2013.

[1] An increased frequency and intensity of winter and spring storms have recently manifested over a broad area of North America—along the east coast of the U.S. especially, though global mean storm tracks are suggested to shift northward. To understand these changes, we have conducted atmospheric model experiments, examining the response of North American storm activity to the elevated tropical Pacific sea surface temperature (SST) associated with El Niño. The results indicate that, when tropical Pacific SST increases, there are more numerous intense storms over southwestern, southeastern, and northwestern North America, but fewer weaker storms over the northeast. Transient eddy analysis of the general circulation demonstrates consistent changes, suggesting systematic changes from large-scale general circulation to synoptic-scale storms. These changes can be attributed to enhanced lower tropospheric baroclinicity, to which the southward shift and an intensification of extratropical jet streams make a major contribution. **Citation:** Basu, S., X. Zhang, I. Polyakov, and U. S. Bhatt (2013), North American winter-spring storms: Modeling investigation on tropical Pacific sea surface temperature impacts, *Geophys. Res. Lett.*, 40, 5228–5233, doi:10.1002/grl.50990.

1. Introduction

[2] Extratropical synoptic-scale cyclonic storms are a fundamental element of daily weather patterns and interactively contribute to large-scale general atmospheric circulation at middle and high latitudes. They can bring blizzards, snowfall, and gusty winds that impact daily life through infrastructure damage and property loss. Storm activities have prominent regional and seasonal structures and exhibit daily to interannual variability [Hoskins and Hodges, 2002; Zhang *et al.*, 2004; Bengtsson *et al.*, 2006]. Storm tracks and activities have also demonstrated a long-term response to changing climate. Recent studies indicate that Northern Hemisphere extratropical storm tracks have shifted poleward and storm activities have intensified in the northern high latitudes and Arctic, and this shift is projected by climate models to continue under global warming scenarios [McCabe *et al.*, 2001; Zhang *et al.*, 2004; Yin, 2005]. Zhang *et al.* [2004] further found that storm activities have distinct regional characteristics across different

geographic sectors, superimposed on the long-term trend of a poleward shift. The variability of storm activity over North America has exhibited a quasi-decadal oscillation [Zhang *et al.*, 2004]. The recently observed intensification of storm activities in North America, in particular along the east coast, would be a manifestation of this regional behavior.

[3] To improve our understanding of such regional variability and changes in storm activities over North America, we have conducted modeling investigations that examine a number of potential forcing factors. One of these factors is the elevated tropical Pacific sea surface temperature (SST) associated with El Niño. Direct and indirect effects of tropical Pacific SST anomalies upon atmospheric circulation and storm tracks have been investigated in several studies. It has been found that jet streams and storm tracks are displaced southward and extended eastward over the eastern Pacific Ocean when tropical Pacific SST increases during El Niño [Trenberth and Hurrell, 1993; Hoerling, 1994; Straus and Shukla, 1997; Zhang and Held, 1999; Orlanski, 2005; Eichler and Higgins, 2006; Compo, 2010]. However, effects of tropical Pacific SST anomalies on storms over the entire North American continent, in particular on recently intensified winter-spring storm activities affecting the east coast, under a climate experiencing accelerated warming, have not yet been fully understood. We will address this problem in this study.

2. Model Experiment Design and Data Analysis Methods

[4] We employed the National Center for Atmospheric Research (NCAR) Community Atmosphere Model (CAM) version 3.1.p2 [Collins *et al.*, 2006; Hurrell *et al.*, 2006]. It was configured at a resolution of T85 (approximately 1.4° for both latitude and longitude), with 26 vertical levels. We conducted two groups of modeling experiments in order to isolate the impacts of elevated tropical Pacific SST on North American storm track dynamics and storm activity: Control Experiments (ConExp) and Sensitivity Experiments (SenExp), which have different surface boundary conditions, defined by SST and sea ice concentration data sets [Hurrell *et al.*, 2008]. To obtain robust results, we performed 60 ensemble runs for each group.

[5] In ConExp, SST and sea ice concentration are prescribed using their long-term climatological monthly means from 1981 to 2001 at each grid point over the global ocean. In SenExp, we constructed elevated tropical Pacific SST using SST data from 1997 to 1998, when a strong El Niño occurred. In particular, we first calculated monthly SST anomalies at each grid point for 1997–1998. Then positive SST anomalies were added to the climatological SST at each grid point over the tropical Pacific region between 10°S and

¹International Arctic Research Center and Department of Atmospheric Sciences, University of Alaska Fairbanks, Fairbanks, Alaska, USA.

²Geophysical Institute and Department of Atmospheric Sciences, University of Alaska Fairbanks, Fairbanks, Alaska, USA.

Corresponding author: X. Zhang, International Arctic Research Center and Department of Atmospheric Sciences, University of Alaska Fairbanks, 930 Koyukuk Dr., Fairbanks, AK 99775, USA. (xdz@iarc.uaf.edu)

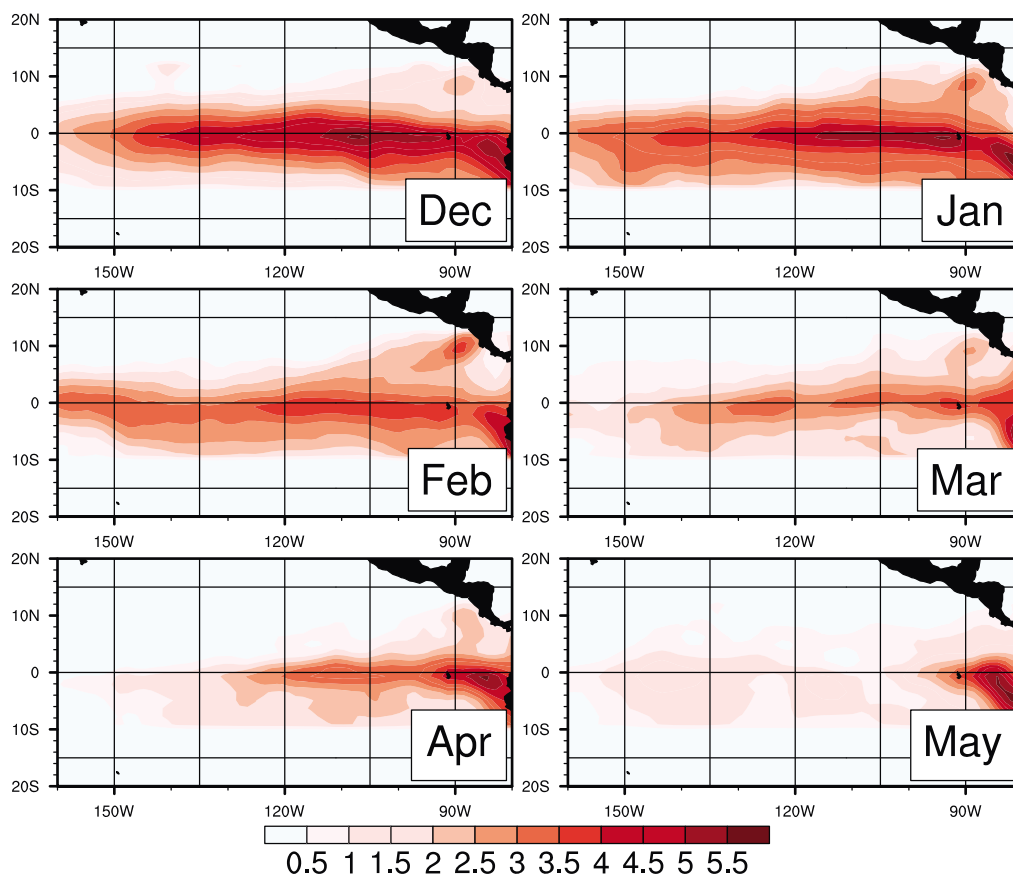


Figure 1. Positive SST anomalies applied to define surface forcing for the sensitivity experiment (SenExp) from December to May.

10°N and from 165°W to 80°W, throughout the simulation time period. The maximum tropical Pacific SST anomaly occurs in December and then gradually decays with time (Figure 1). Climatological monthly SST data was specified for grid points outside this tropical Pacific region. Climatological sea ice concentration was specified at the sea ice covered grid points in both the Northern and Southern Hemispheres.

[6] All ensemble runs for both ConExp and SenExp were carried out from 1 November to 31 May, with 6-hourly output of selected variables. We allowed 1 month for the model to spin up, and we used model results from December to the following May. To analyze storm activities in both experiments, we applied a storm identification and tracking algorithm [Zhang *et al.*, 2004] to the 6-hourly sea level pressure (SLP) outputs from each model ensemble. This algorithm identifies a low SLP center, which should have a minimum SLP gradient of at least 0.15 hPa per 100 km with surrounding grid points and should survive for more than 12 h. More details about this algorithm and its application for investigating Northern Hemisphere storm track variability and changes can be found in Zhang *et al.* [2004]. In addition, considering the distinct geographical features and greater climatological storm activity near the coasts, we divided the North American continent into four subregions in this study (Figure 2).

3. Results

3.1. Changes in North American Storm Activity

[7] The storm identification and tracking algorithm provides parameters that describe various aspects of storm

activity, including duration or lifetime, central location, and central SLP, for each individual storm occurring over the study area. By using the data sets of these parameters from each ensemble run of ConExp and SenExp, we derived the number of storm trajectories, mean storm duration, and mean storm intensity for each subregion in both winter (December–February) and spring (March–May). Following Zhang *et al.* [2004], storm trajectory is defined from the time of storm generation until dissipation within the study area, or from the time when the storm enters the study area until the time it leaves the study area. Mean duration for each subregion is the average duration for the total number of storm trajectories within the study area. The storm intensity for individual storms was calculated as the difference between the storm’s central SLP and the monthly mean SLP at the corresponding location. Mean intensity for each subregion was obtained by averaging storm intensities over their duration and over all storm trajectories.

[8] We conducted a statistical analysis for all 60 ensembles in both ConExp and SenExp. Probability density functions (PDFs) of the number of trajectories, mean intensity, and mean duration exhibit various differences in climate features of storm activity between ConExp and SenExp, over each of the subregions and during both winter and spring (Figure 3). In both ConExp and SenExp, the number of storm trajectories shows a Gaussian distribution over the subregions in winter and spring, except for a bimodal distribution over southwestern North America (SWNA) during winter. Noticeable seasonality is present in the PDFs for both groups of experiments. In ConExp, the peak frequency generally increases and shifts to a

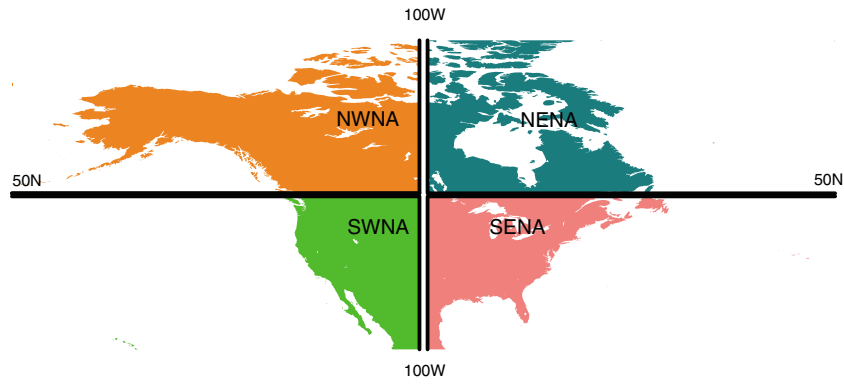


Figure 2. The four subregions used in this study: southwestern North America (SWNA) (20°N–50°N, western coastline to 100°W), southeastern North America (SENA) (20°N–50°N, 100°W to Eastern coastline), northwestern North America (NRNA) (50°N–80°N, western coastline to 100°W), and northeastern North America (NENA) (50°N–80°N, 100°W to Eastern coastline).

higher number of trajectories from winter to spring over SWNA and southeastern North America (SENA), suggesting more numerous storms in spring in these two subregions. An increase and a decrease in peak frequency occur for the trajectories over northwestern North America (NRNA) and northeastern North America (NENA), respectively.

[9] Comparison between ConExp and SenExp indicates noticeable changes in the numbers of storm trajectories when tropical Pacific SST increases. In addition to significant increases based on the Student’s *t* test, peak frequencies over

SWNA and SENA also shift toward a higher number of storm trajectories, from 51 ± 6 and 62 ± 6 to 57 ± 7 and 69 ± 6 during winter (Figures 3a and 3b). Peak frequencies show a slight decrease in spring, and no obvious shift occurs within these two subregions. In NRNA, peak frequencies exhibit a shift to a higher number of trajectories in both winter and spring (Figure 3c). However, a decrease occurs in the NENA region (Figure 3d). Note that interconnections may exist in storm frequencies between the subregions, though the analysis here mainly focuses on storm activities in each subregion. For

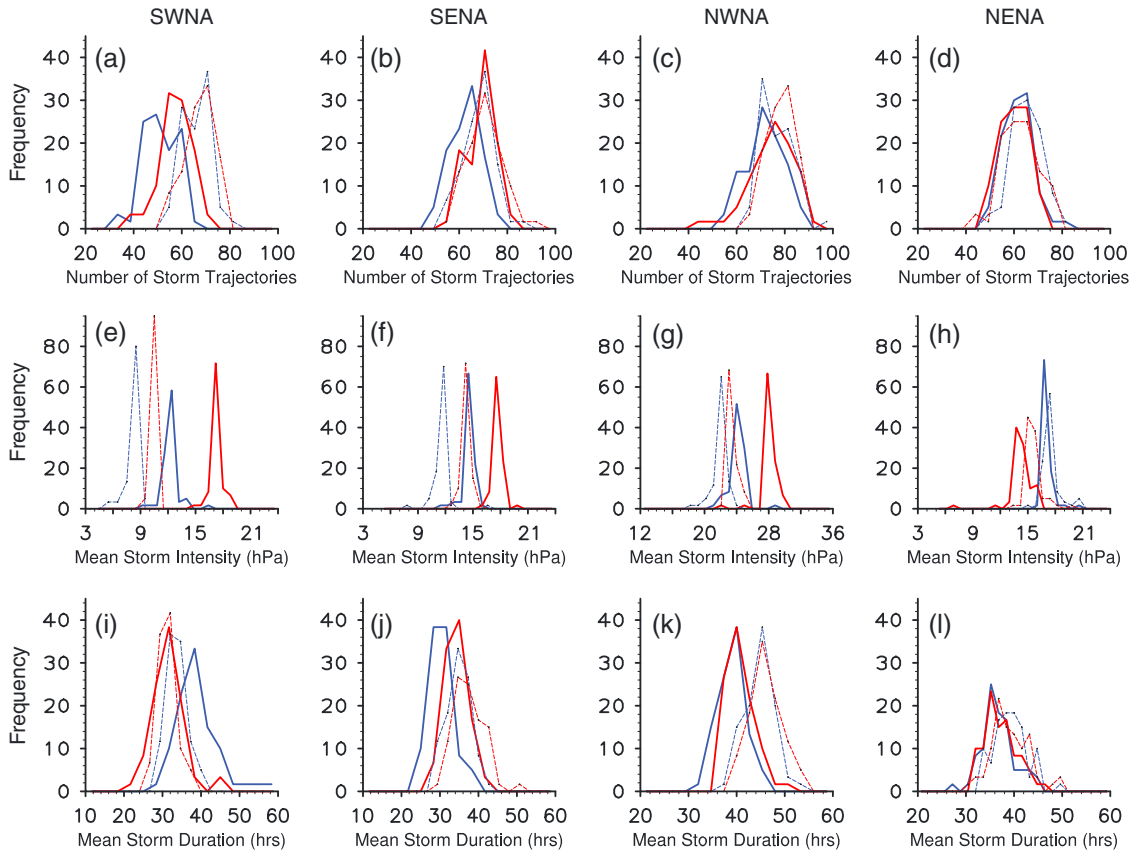


Figure 3. Probability density functions (PDFs) of (a–d) the number of storm trajectories, (e–h) the mean storm intensity, and (i–l) the mean duration for the four subregions in winter (solid lines) and spring (dashed lines). The blue (red) color represents the results from the ConExp (SenExp).

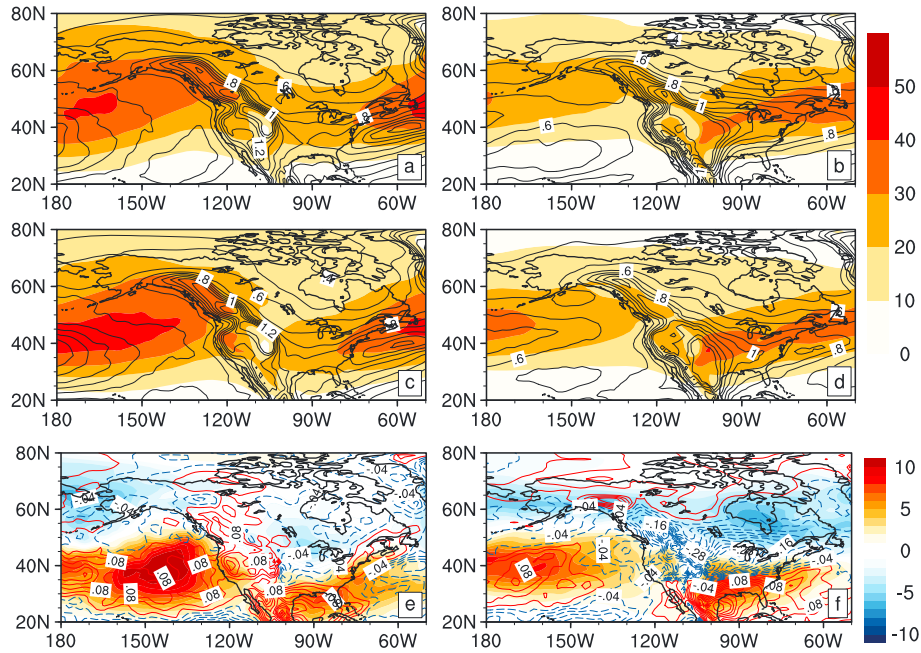


Figure 4. Transient eddy kinetic energy (KJ/m^2 , shaded) and superimposed Eady Growth Rate Maximum (day^{-1} , contours) at 775 hPa in ConExp for (a) winter and (b) spring. (c and d) The same as Figures 4a and 4b, but for SenExp. The differences between SenExp and ConExp are displayed for (e) winter and (f) spring.

example, storms, that are generated in or travel to the western U.S., may continually enter the eastern U.S. So, the increased number of storm trajectories in the western U.S. may also contribute to the increase in the eastern U.S.

[10] Climatologically, storm intensity is generally characterized by a narrow, Gaussian-like distribution in all subregions and in both winter and spring, according to the simulations in ConExp (Figures 3e–3h). Storms are stronger in winter and get weaker in spring in most subregions, except for an opposite seasonal variation in NENA. The PDFs of intensity show a similar distribution in SenExp. However, when comparing intensities between ConExp and SenExp, we can readily find significant intensification of storms over most subregions, with maximum frequency shifting from a mean intensity of 12.21 ± 0.95 (8.17 ± 0.68) to 17.33 ± 0.61 (10.35 ± 0.23) hPa over SWNA; 14.59 ± 0.72 (11.56 ± 0.93) to 17.65 ± 0.52 (14.11 ± 0.49) hPa over SENA; and 24.15 ± 0.96 (21.90 ± 0.86) to 28.13 ± 1.01 (23.43 ± 0.60) hPa over NENA in winter (spring). Similar to its seasonal variation, storm intensity noticeably decreases over NENA in winter and spring with increased tropical Pacific SST.

[11] Storms generally have longer duration over the western half of the North American continent than the eastern half, as characterized by their PDFs in Figures 3i–3l. In response to increased tropical Pacific SST, SWNA storms show a decrease in durations from 38.71 ± 5.59 (33.43 ± 2.72) to 31.22 ± 4.05 (31.22 ± 2.47) h in winter (spring), as shown by the comparison of peak frequencies of PDFs between ConExp and SenExp. In contrast, storms over SENA exhibit prolonged mean durations, from 30.23 ± 3.02 (34.66 ± 3.14) to 34.48 ± 3.0 (37.51 ± 3.86) h in winter (spring). Nevertheless, no obvious changes are found in storm durations over NENA and NENA in SenExp. It is worth mentioning that the duration depends on moving speed of storms within each subregion. So storms can carry the same moving features from one subregion to another, impacting mean durations in two study areas.

[12] Statistical analysis across all ensembles of ConExp and SenExp indicates systematic changes in different aspects of storm activity over North America. When tropical Pacific SST increases, there are more numerous, more intense storms over SWNA, SENA, and NENA, i.e., the entire U.S. continent, as well as western Canada and Alaska. The storms over SENA, i.e., the eastern U.S., demonstrate longer duration or lifetime than their climatology. To better understand the physical processes and mechanisms behind these changes, we will further examine these synoptic-scale storm activities in the context of the large-scale atmospheric general circulation in the following section.

3.2. Perspective From Large-Scale Circulation and Associated Physical Mechanisms

[13] In the above analysis, we employed a Lagrangian approach to identify and track each storm. To link detected storm activities to the atmospheric general circulation, we conducted further analysis by using a Eulerian method to represent overall storm activities at each grid point. Specifically, we computed transient eddy kinetic energy (EKE, KJ/m^2) at each grid point at 775 hPa, defined as

$$\text{EKE} = \frac{1}{2} (u'^2 + v'^2) \quad (1)$$

where u' and v' are the high pass (≤ 6 days) filtered data for a consistency with the analysis above using the Lagrangian approach that used 6-hourly based data. Considering upstream origins of storms impacting North America, our computation and analysis area extend to include the western North Pacific. Figures 4a–4d show the EKE from the two groups of simulations, ConExp and SenExp, for winter and spring, respectively.

[14] In climatology simulated by ConExp, large EKE occurs from the middle and eastern North Pacific to the Bering Strait

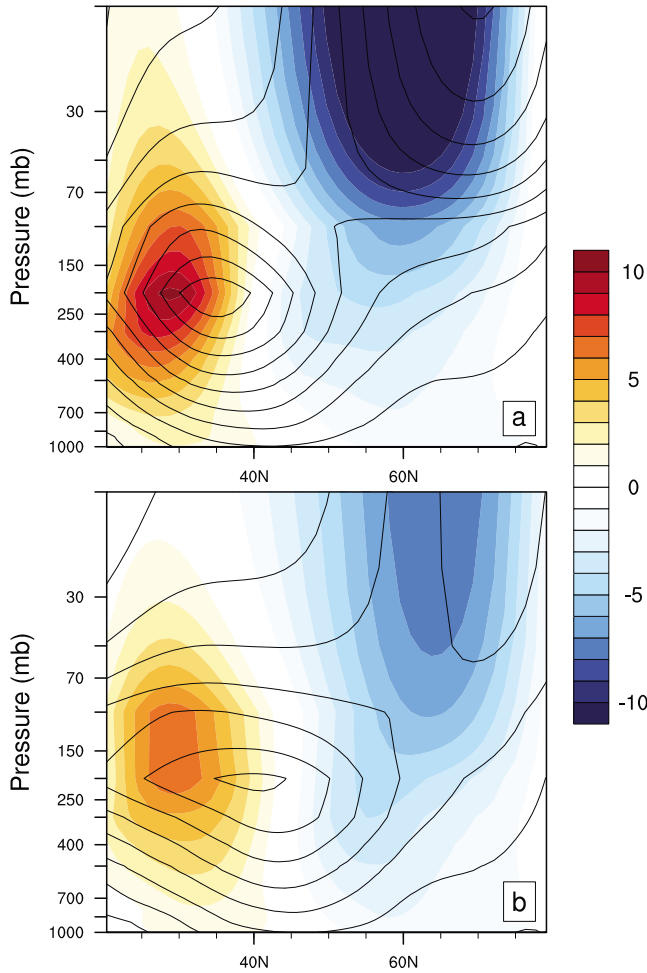


Figure 5. Zonally averaged (between 180° and 310°) climatological zonal wind (contours) and the differences between SenExp and ConExp (shaded) across the vertical section along 20°N – 80°N for (a) winter and (b) spring.

and the interior Alaska in winter. Maximum EKE appears over the Aleutian Islands. Another large wintertime EKE area includes most of the North American continent east of the Rocky Mountains and the North Atlantic coast. These large EKE distributions are in good agreement with climatological winter storm tracks [e.g., Zhang *et al.*, 2004; Bengtsson *et al.*, 2006]. EKE also demonstrates seasonal variations, showing considerable decreases from winter to spring (comparing Figures 4a versus 4b), consistent with the storm intensity analysis shown in the previous sections.

[15] Changes in EKE forced by the increased tropical Pacific SST can be easily identified when comparing simulations between ConExp and SenExp (Figure 4). The Aleutian maximum of EKE is dramatically shifted southeastward, to the northeastern North Pacific, in both winter and spring, in spite of large seasonal differences in their magnitude. These changes also exhibit an increase in storm activities along the west coast and extending to the Rocky Mountains. Another pronounced increase occurs from the middle U.S. to the east coast, in particular for the spring season. Each of these EKE changes corresponds well to the intensity changes shown by the PDFs in Figures 3e–3h.

[16] Why do changes occur in the EKE or storm activities in response to increased tropical Pacific SST forcing? To

answer this question, we quantitatively examined the Eady Growth Rate Maximum (EGRM, day^{-1}) at 775 hPa for each ensemble of the ConExp and SenExp. The EGRM is given by Hoskins and Valdes [1990] as

$$\text{EGRM} = 0.31 f \left| \frac{\partial U}{\partial z} \right| N^{-1} \quad (2)$$

where f is the Coriolis parameter, N is the Brunt Väisälä Frequency, and U is the horizontal wind vector. EGRM depends on vertical wind shear and atmospheric static stability and is usually calculated at the lower levels of the atmosphere, where major baroclinic development occurs. It measures the intensity of atmospheric baroclinic instability, which is the principle mechanism supporting extratropical storm development.

[17] Climatological wintertime EGRM for ConExp demonstrates large values mainly over three areas, including the North Pacific, the west coast and Rocky Mountains of the U.S., and the east coast of the U.S. (the contours in Figure 4a), suggesting strong baroclinicity in these areas for storm generation and development. In spring, climatological EGRM considerably decreases (Figure 4b). Although the primary spatial structures of EGRM in SenExp are very similar to those of ConExp, differences can be found in a comparison between Figures 4e and 4f. An increase in EGRM occurs in SenExp over the eastern North Pacific and along the U.S. west coast, from southeastern Alaska to California, in both winter and spring. This increase also occurs over the area from the southeastern U.S. and the Gulf of Mexico to the east coast in both seasons. In spring, the increase in EGRM extends considerably northward to the central and eastern United States. A decrease occurs from the lee side of the Rocky Mountains to the east coast of Canada. These changes in EGRM are consistent with and provide dynamic support for the spatial shift of storm tracks identified by the tracking algorithm and transient eddy analysis described above.

[18] Vertical wind shear is a primary contributor to the EGRM and its changes. We therefore analyzed the vertical structure of the zonal wind averaged between 180° and 310° longitude in both SenExp and ConExp for both winter and spring (Figure 5). The results indicate a strengthening and southward shifting of the subtropical jet stream, particularly in winter, when the tropical Pacific SST increases in SenExp compared to its climatology in ConExp. The changes in the jet stream identified here are consistent with previous findings that elevated tropical Pacific SST can force an intensified and southward contracted Hadley Cell over the eastern Pacific [e.g., Lu *et al.*, 2008]. The changed jet stream between 25°N and 40°N can result in an increase in EGRM further southward than its climatology and, in turn, supports the intensified and southward shifted storm tracks found above. In addition, the jet stream favors storms developing on its south side, due to the associated large upper-level divergence. When further examining large-scale circulation, we found that the difference of 500 hPa geopotential height between SenExp and ConExp shows a PNA-like pattern (not shown), with intensified low pressure systems over the Aleutian Islands and the southeastern U.S. and anomalous high pressures over the northeastern U.S. and eastern Canada. The northwest-to-southeast aligned background steering flow favors storms to propagate to the southeastern U.S.

4. Concluding Remarks

[19] An increased frequency of intense storms has been observed in North America, in particular along the east coast area. We have employed the community atmospheric model NCAR CAM 3.1 to conduct two groups of modeling experiments. Statistics derived by a storm identification and tracking algorithm (a Lagrangian approach) [Zhang *et al.*, 2004] show a distinct seasonality and significant changes in storm activities. In climatology, the number of storm trajectories increases, though intensity decreases from winter to spring over southwestern, southeastern, and northwestern North America. There is also an increase in the number of storm trajectories, though little change in intensity during winter and spring in northeastern North America. When tropical Pacific SST increases, model experiments suggest a significantly increased number and intensity of storms over the southwest, southeast, and northwest, i.e., the entire U.S., as well as western Canada and Alaska, during winter and spring. However, less and weaker storms occur over northeastern North America in both seasons. This suggests a southward shift of storm tracks over the eastern U.S. Meanwhile, storms over southeastern North America, i.e., the eastern U.S., demonstrate a longer duration or lifetime than their climatology.

[20] To better understand these changes in storm activities, we investigated, for the first time, the linkage between surface storms identified by the Lagrangian approach and transient eddies in general circulation computed by Eulerian approach and measured by EKE. Changes in surface storm tracks and activity over North America are consistent with those in EKE, which are attributed to changed baroclinicity. When tropical Pacific SST increases, maximum EGRM shifts south-eastward from the Aleutian Islands to western North America, particularly in winter. Considerably increased EGRM occurs from southeastern Alaska and western Canada to California. EGRM also increases substantially from the southern U.S. to the east coast, with the largest increase in spring. The southward shift and intensification of the subtropical jet stream favor an increase in vertical wind shear in the lower troposphere to the south of the climatological jet stream, contributing to increasing baroclinicity, enhancing air mass divergence, and, in turn, supporting surface storm development and strengthening. Meanwhile, the PNA-like pattern and associated northwest-to-southeast alienated background flow favor storms to propagate to the southeast U.S.

[21] An increase in storm events in a warming climate has significant implications for human society and the natural environment. Recent observations have shown an increasing tendency of frequency and intensity of El Niño [e.g., Cobb *et al.*, 2013], although there are still uncertainties in climate model projections in a future warming climate [e.g., Collins *et al.*, 2010]. Results from this study would help improve understanding, enhance predictive capability, and reduce future projection uncertainties of storm events over North America under the scenario of a changed El Niño, induced by global

warming forcing, which is important for policy decision-making processes.

[22] **Acknowledgments.** We are grateful to the Editor and the anonymous reviewer for their constructive comments and suggestions, which improved content and presentation of this paper. We thank Nicole Mölders for serving on Soumik Basu's advisory committee and providing valuable suggestions and comments. We also thank NCAR for making CAM available and the Arctic Region Supercomputing Center for providing computational resources. This study is supported by the NOAA grant NA06OAR4310147 and the grant to the University of Alaska Fairbanks, International Arctic Research Center from the Japan Agency for Marine-Earth Science and Technology (JAMSTEC) under the "JAMSTEC and IARC Collaboration Studies."

[23] The Editor thanks an anonymous reviewer for their assistance in evaluating this paper.

References

- Bengtsson, L., K. I. Hodges, and E. Roeckner (2006), Storm tracks and climate change, *J. Clim.*, *19*, 3518–3542.
- Cobb, K. M., N. Westphal, H. R. Sayani, J. T. Watson, E. Di Lorenzo, H. Cheng, R. L. Edwards, and C. D. Charles (2013), Highly variable El Niño-Southern Oscillation throughout the holocene, *Science*, *339*, 67–70, doi:10.1126/science.1228246.
- Collins, W. D., P. J. Rasch, B. A. Boville, J. J. Hack, J. R. McCaa, D. L. Williamson, B. P. Briegleb, C. M. Bitz, S.-J. Lin, and M. Zhang (2006), The formulation and atmospheric simulation of the Community Atmosphere Model Version 3 (CAM3), *J. Clim.*, *19*, 2144–2161.
- Collins, M., et al. (2010), The impact of global warming on the tropical Pacific Ocean and El Niño, *Nat. Geosci.*, *3*, 391–397, doi:10.1038/ngeo868.
- Compo, G. P. (2010), Removing ENSO related variation from climate record, *J. Clim.*, *23*, 1957–1978.
- Eichler, T., and W. Higgins (2006), Climatology and ENSO-related variability of North American extratropical cyclone activity, *J. Clim.*, *19*, 2076–2093.
- Hoerling, M. P. (1994), Organization of extratropical transients during El Niño, *J. Clim.*, *7*, 745–766.
- Hoskins, B. J., and K. I. Hodges (2002), New perspective on the Northern Hemisphere winter storm tracks, *J. Atmos. Sci.*, *59*, 1041–1061.
- Hoskins, B. J., and P. J. Valdes (1990), On the existence of storm tracks, *J. Atmos. Sci.*, *47*, 1854–1864.
- Hurrell, J. W., J. J. Hack, A. S. Phillips, J. Caron, and J. Yin (2006), The dynamical simulation of the Community Atmosphere Model Version 3 (CAM3), *J. Clim.*, *19*, 2162–2183.
- Hurrell, J. W., J. J. Hack, D. Shea, J. M. Caron, and J. Rosinski (2008), A new sea surface temperature and sea ice boundary dataset for the Community Atmosphere Model, *J. Clim.*, *21*, 5145–5152.
- Lu, J., G. Chen, and D. M. W. Frierson (2008), Response of the zonal mean atmospheric circulation to El Niño versus global warming, *J. Clim.*, *21*, 5835–5851.
- McCabe, G. J., M. P. Clark, and M. C. Serreze (2001), Trends in Northern Hemisphere surface cyclone frequency and intensity, *J. Clim.*, *14*, 2763–2768.
- Orlanski, I. (2005), A new look at the Pacific storm track variability: Sensitivity to tropical SSTs and to upstream seeding, *J. Atmos. Sci.*, *62*, 1367–1390.
- Straus, D. M., and J. Shukla (1997), Variations of midlatitude transient dynamics associated with ENSO, *J. Atmos. Sci.*, *54*, 777–790.
- Trenberth, K. E., and J. W. Hurrell (1993), Decadal atmosphere-ocean variations in the Pacific, *Clim. Dyn.*, *9*, 303–319.
- Yin, J. H. (2005), A consistent poleward shift of the storm tracks in simulations of 21st century climate, *Geophys. Res. Lett.*, *32*, L18701, doi:10.1029/2005GL023684.
- Zhang, Y., and I. M. Held (1999), A linear stochastic model of a GCM's midlatitude storm tracks, *J. Atmos. Sci.*, *56*, 3416–3435.
- Zhang, X., J. E. Walsh, J. Zhang, U. S. Bhatt, and M. Ikeda (2004), Climatology and interannual variability of Arctic cyclone activity: 1948–2002, *J. Clim.*, *17*, 2300–2317.